



HAL
open science

Effusive and explosive volcanism on the northern Futuna Ridge, Lau Basin: A combined bathymetric, magnetic and seismic investigation

Florent Szitkar, Jérôme Dymont, Ewan Pelleter, Yannick Thomas, Bruno Marsset, Stephan Ker, Yves Fouquet

► To cite this version:

Florent Szitkar, Jérôme Dymont, Ewan Pelleter, Yannick Thomas, Bruno Marsset, et al.. Effusive and explosive volcanism on the northern Futuna Ridge, Lau Basin: A combined bathymetric, magnetic and seismic investigation. *Journal of Volcanology and Geothermal Research*, 2022, 431, 10.1016/j.jvolgeores.2022.107646 . insu-03776396

HAL Id: insu-03776396

<https://insu.hal.science/insu-03776396>

Submitted on 13 Sep 2022

HAL is a multi-disciplinary open access archive for the deposit and dissemination of scientific research documents, whether they are published or not. The documents may come from teaching and research institutions in France or abroad, or from public or private research centers.

L'archive ouverte pluridisciplinaire **HAL**, est destinée au dépôt et à la diffusion de documents scientifiques de niveau recherche, publiés ou non, émanant des établissements d'enseignement et de recherche français ou étrangers, des laboratoires publics ou privés.



Distributed under a Creative Commons Attribution 4.0 International License



Effusive and explosive volcanism on the northern Futuna Ridge, Lau Basin: A combined bathymetric, magnetic and seismic investigation

Florent Szitkar^{a,*}, Jérôme Dymet^b, Ewan Pelleter^c, Yannick Thomas^c, Bruno Marsset^c, Stephan Ker^c, Yves Fouquet^c

^a The Geological Survey of Norway (NGU), Trondheim, Norway

^b Université Paris Cité, Institut de physique du globe de Paris, CNRS, Paris, France

^c Ifremer, Unité Géosciences Marines, 29280 Plouzané, France

ARTICLE INFO

Keywords:

Volcaniclastic domes
Volcanic edifices
Futuna Ridge
Magnetics
Seismics
Bathymetry

ABSTRACT

The Utu Uli Hill, located on the northern Futuna Ridge in the Lau Basin (Southwestern Pacific Ocean), displays recent volcanism in a complex area, possibly the boundary of one of many intermediate platelets between the Pacific and Australian plates or the result of progressive melting and dismantling of the Vitiaz subduction slab. The combination of bathymetric, magnetic and 3D reflection seismic data allows us to recognize and describe several types of submarine volcanoes, namely clustered small volcanoes, flat-topped volcanoes, elongated volcanic ridges, and volcanoclastic domes, and to unravel the geological evolution of the area. Sea-surface magnetic anomalies reveal that the area formed during the last 780 ka, whereas the large variations of amplitude in the near-seafloor, high-resolution magnetic anomalies suggest scattered ages for individual edifices and widespread volcanism within the whole Futuna Ridge. The spectacular volcanoclastic domes initiate only at depth shallower than 1150–1200 m. They show feeder dyke systems and evidence of hydrothermalism at their summit, and are locally affected by collapse structures.

1. Introduction

A large part of submarine volcanism occurs on mid-ocean ridges, at depth >2000 m, where the water column pressure usually prevents explosive manifestation such as pyroclastic eruptions or lava fountains (e.g., Fisher, 1984). As a result, the corresponding seafloor is mostly paved by pillow lavas and other lava flows, lacking the diversity of volcanic provinces on land. Explosive eruptions and volcanoclastic deposits have however been reported at depth of ~4000 m on ultraslow spreading centers (Gakkel Ridge at Oden volcano: Sohn et al., 2008) as a possible consequence of volatile gas accumulation at depth, in a context of long intervals between eruptions. In shallow submarine areas such as mid-ocean ridges close to hotspots, back-arc basins, volcanic arcs, and hotspot seamount chains, submarine explosive volcanism is well documented and has been directly observed (for instance on the Mid-Atlantic Ridge near the Azores: Menez Gwen, Fouquet et al., 1998; Eissen et al., 2003; in the Mariana back arc spreading center: NW Rota 1, Chadwick, 2008; and in the Lau Basin: West Mata, Clague et al., 2011; Embley et al., 2014). In this paper, we present a unique set of high-resolution

bathymetric, magnetic and 3D reflection seismic data acquired in a relatively shallow volcanic area of the Lau basin, the Futuna Ridge, in the Exclusive Economic Zone of the French Overseas Territory of Wallis et Futuna. Several distinct types of volcanic features are observed: clustered small volcanoes and flat-topped volcanic edifices, both with a basaltic structure and limited sediment cover, elongated volcanic ridges, and volcanoclastic domes mostly made of volcanoclastic sediments supported by a skeleton of feeder dykes. We describe the bathymetric, magnetic and seismic character of these features and try to unravel the age and evolution of the area, marked by widespread volcanism over the possible boundary of another Lau Basin platelet and/or a volcanic ridge related to the demise of the dismantled Vitiaz slab (Szitkar et al., 2020).

2. Regional geological context

The North Fiji and Lau basins, at the limit of the Australian and Pacific plates, define a complex area made of several transient microplates bounded by discrete or diffuse active volcanic areas (e.g., Szitkar et al., 2020). The Futuna Plate is separated from the Pacific Plate by the

* Corresponding author.

E-mail address: florent.szitkar@ngu.no (F. Szitkar).

<https://doi.org/10.1016/j.jvolgeores.2022.107646>

Received 16 June 2022; Received in revised form 7 August 2022; Accepted 9 August 2022

Available online 13 August 2022

0377-0273/© 2022 The Authors. Published by Elsevier B.V. This is an open access article under the CC BY license (<http://creativecommons.org/licenses/by/4.0/>).

North-South Futuna Ridge (Pelletier et al., 2001), to the west, and by a complex set of transform faults along which transpressional motion has resulted in the emergence of Futuna Island (Pelletier et al., 2000), to the north. Between 15°40'S (immediately North of Vanua Levu, in Fiji Islands) and 14°30'S, the Futuna Ridge exhibits the morphology of a spreading center, marked by a deep axial valley south of 15°10'S and an axial dome north of 14°50'S. North of 14°30'S, the continuous spreading center becomes a set of left-lateral *en-échélon* N35°E ridges, some of them connecting to the West Futuna Island Transform Fault. Surprisingly, the *en-échélon* ridge system continues northward, between 14°05'N and 13°47'S, where the 7 to 13 km-wide, 40 km-long N35°E volcanic ridge culminates at 440 m below sea level (bsl) (Fig. 1A).

The plate tectonic role of this ridge is still elusive. It may correspond to a plate boundary continuing in a N80°E graben and possibly abutting the former Vitiaz subduction zone, defining another microplate north of the Futuna Plate. Conversely, it may also be one of the volcanic ridges observed south of the Vitiaz Trench, such as the Rotuma Ridge or the off-axis Horizon Bank, abutting segment TR3 of the Tripartite Ridge and SPR1 of the South Pandora Ridge, respectively (Lagabrielle et al., 1996). These ridges most likely result from the progressive melting and dismantling of the Vitiaz subduction slab (Sztikar et al., 2020).

In this study, we focus on the volcanic Utu Uli Hill, located at 13°50'S, 178.47°W, near the northern end of the Futuna Ridge (Fig. 1A, B). The hill is about 4 km-long and 2 km-wide, and displays an average

N50°E orientation, underlining the progressive change of the structural trend from N35°E along the Futuna Ridge to N80°E in the graben eastward (Fig. 1B). It has been surveyed as part of the FUTUNA cruise series, which aimed at assessing the deep-sea mineral potential of the Wallis-and-Futuna EEZ. Ni-Cu-Co-rich hydrothermal manganese mineralization have been discovered near the Utu Uli Hill summit (Pelletier et al., 2017).

High-resolution bathymetry acquired ~70 m above seafloor (asf) with an Autonomous Underwater Vehicle (AUV) reveals contrasting morphologies (Fig. 1C). The southeastern part of the survey displays volcanic edifices of various size, from decametric to kilometric, often superimposed, characteristic of relatively fresh basaltic seafloor. Conversely, the northwestern part shows a remarkably smooth topography, suggesting an important sedimentary cover. The Utu Uli Hill lies between these two areas. The hill is made of a rather smooth central part, topping at 890 m bsl, and overlooks the volcanic southeastern area by ~400 m, whereas the northwestern area constitutes the western slope of the Futuna Ridge over >1000 m depth. The central part is made of several coalescent domes, possibly three domes to the northeast and two to the southwest. Further northeast (respectively southwest), the Utu Uli Hill morphology turns to two (resp. one) elongated volcanic ridges marked by a rougher morphology. Additional features of interest include collapse structures, the first one displaying a clear horseshoe shape at the western edge of the survey, the two others showing slid blocks of

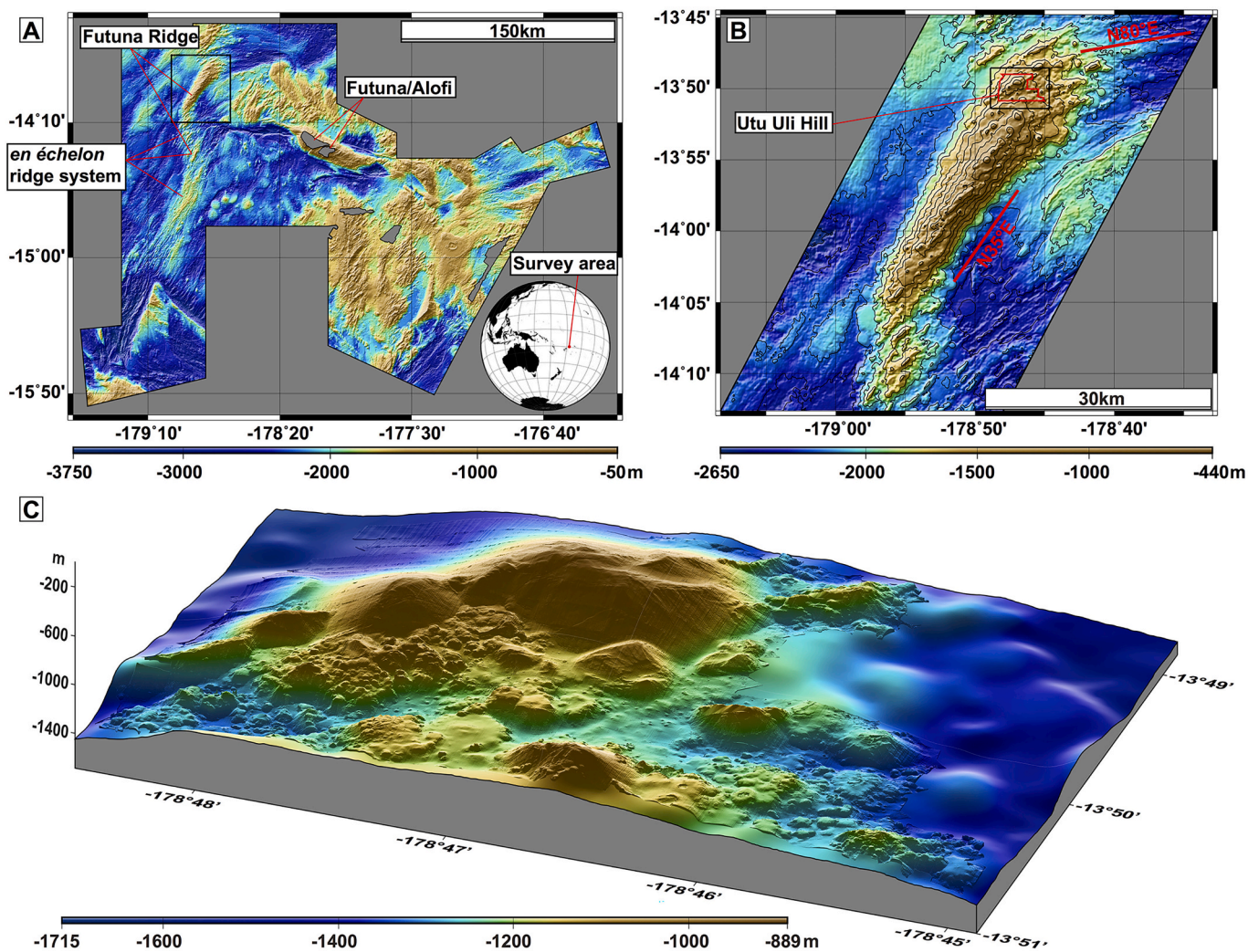


Fig. 1. (A) Regional, ship-based bathymetry around Futuna Island. The survey area is located West of the island. (B) Close-up on the northernmost part of the Futuna Ridge. The Utu Uli Hill stands next to the northern end of this ridge. (C) 3D projection of the high-resolution bathymetry acquired ~70 m asf by AUV Aster^x during cruise FUTUNA 1 above the Utu Uli Hill. No vertical exaggeration.

coherent sediments at the foot of the central part (Fig. 2A, B, C).

Direct geological observations have also been carried out onboard Deep-Sea manned Vehicle (DSV) *Nautilus* and the surface and subsurface rocks have been sampled by various types of coring systems at maximum depth of 1.5 m. Direct observations confirm the basaltic seafloor with locally thin pelagic sediment cover south of the central part of the Hill and on the elongated ridges that extend the Utu Uli Hill to the northeast and southwest, as anticipated from the morphology (see Supplementary Fig. 1 for the location of the dives). The other sections of the dives revealed pyroclastic sediments covered by hydrothermal manganese crusts and, near the summit of the Utu Uli Hill, “layered crusts with bread-crust-like fractures” and “iron and silica-rich crests and/or veins” of metric size, which “likely reflect pulses of hydrothermal activity” (Pelletier et al., 2017). Coring confirms the presence of hydrothermal precipitates (iron and manganese oxyhydroxides, nontronite). Although of great interest for metallogeny and mineral resources, understanding the hydrothermal processes of this system at shallow depth is beyond the scope of this paper and will be the topic of another publication.

3. Magnetic and seismic data

Magnetic data were collected at three different scales and resolution in the Utu Uli area. Regional magnetic surveys at sea-surface were obtained by R/V *L'Atalante* along East-West tracks in 2000 (cruise ALAUF1) and along N35°E tracks in 2010 (cruise FUTUNA 1). The total magnetic field data have been corrected for the International Geomagnetic Reference Field (Alken et al., 2021) to obtain scalar magnetic anomaly.

The Utu Uli Hill has been surveyed at a 70 m altitude asf by AUV *Aster^X* in 2010 (cruise FUTUNA 1), which collected vector magnetic data along 19 East-West profiles 195 m apart. The AUV data processing is described in Sztikar et al. (2016) and in the Supplementary Information. The resulting equivalent magnetization and Reduced-To-the-Pole (RTP) magnetic anomaly maps are shown in Fig. 3.

High-resolution 3D reflection seismic data have been acquired on the Utu Uli Hill in 2011 (cruise FUTUNA2) to better characterize the volcanoclastic sediment layer and the hydrothermal processes therein. To achieve 3D High Resolution seismic imaging, two 48-channel, 350 m-long streamers were operated 25 m apart with a dual seismic source, 12.5 m apart, shooting alternatively every 3 s. The homogenous coverage of the 21 km² (3.5 km × 6 km) survey area required the acquisition of 176 seismic lines separated by 25 m: 140 nominal lines, plus 36 infill lines. The use of small volume mini-GI air-guns and shallow depth for towing both sources and streamers result in a repetitive impulse seismic signature with a 110 Hz dominant frequency. The geometry of the seismic device and the resulting spatial sampling allow 3D seismic imaging at this frequency content. After careful editing for noise, source defaults, and tidal correction, 16 million recorded traces were 3D-stacked using a bin size of 6.25 × 6.25 m² with a mean fold of 23. A two step 2D migration was then applied (Thomas et al., 2012) to produce the final seismic volume characterized by a 3 m vertical resolution and 15 to 25 m lateral resolution. Both stack and migration processing were achieved using a constant velocity. The short length of the streamers with respect to the water depth does not allow us to infer seismic velocities. This approximation results in a loss of lateral resolution. As previously mentioned, we do not describe the shallow subsurface structures (< 20 m) related to hydrothermalism, but restrict our use of the seismic data to investigate the basement, volcanic features, and other large scale structures.

4. Results

4.1. Magnetism

The East-West sea-surface scalar magnetic anomaly profiles collected during cruise ALAUF1 consistently show ~50 km-wide axial magnetic anomalies along the Futuna Ridge south of 14°20'S (Pelletier et al.,

2001). These anomalies imply an average spreading rate of 32 km/My for the last 0.78 million years. Further north, the axial anomaly is difficult to identify over the *en-echelon* volcanic ridges. The shallow volcanic ridge north of 14°05'S presents a much narrower, ~10 km-wide, positive magnetic anomaly that closely mimic the topography. The deeper seafloor surrounding this ridge does not show consistent parallel anomalies that may be interpreted as older isochrons, resulting in an ambiguous interpretation of the positive anomaly associated with the shallow ridge, which can either represent a complete Anomaly 1 formed at a slow spreading rate (9 to 17 km/My) or a partial Anomaly 1 formed at a faster rate. The important point for our study is that the Utu Uli Hill is clearly located within the positive magnetic anomaly, i.e. it formed within Anomaly 1 (Brunhes polarity interval, since 0.78 Ma following the geomagnetic polarity time scale of Cande and Kent, 1995).

The high-resolution RTP magnetic anomaly map over the Utu Uli Hill reflects the major contrast observed between basalt and sediment areas. In general, areas displaying volcanic morphologies are associated with magnetic anomalies of high amplitudes (16,000 nT peak to peak) and a wide range of wavelengths (200 to 2000 m), whereas the areas covered by volcanoclastic sediments show anomalies of low amplitudes (3200 nT peak to peak) and long wavelengths (700 to 2000 m). This observation is consistent with the volcanoclastic sediments bearing a weak magnetization, the clasts showing random orientation and the magnetization of magnetic minerals cancelling out. The volcanoclastic sediment layer therefore plays the role of a non-magnetized screen, the lower amplitude and longer wavelength anomalies in the sedimented area reflecting the increased distance between the underlying magnetized basaltic basement and the magnetometer sensor.

In the southeastern volcanic seafloor area, bathymetric highs (respectively lows) generally correspond to positive (resp. negative) RTP anomalies (Fig. 3D). This observation may reflect two non-exclusive causes: either systematic variations in the distance between the magnetic basaltic seafloor and the magnetometer sensor, or a stronger magnetization of the protruding volcanic edifices. Systematic variations in the distance between the magnetic seafloor and the sensor may result from two effects: the thicker pelagic sediment accumulation in the bathymetric lows and the navigation of the AUV. Over bathymetric highs (resp. lows), the AUV tends to fly closer (resp. further away) to the seafloor than its nominal altitude of 70 m. A careful analysis of the AUV altitude during the survey reveals, however, that the AUV tends to fly higher (resp. lower) than its nominal altitude when ascending (resp. descending) bathymetric highs (Supplementary Fig. 2). In order to test whether the observed anomalies in the southeastern area are caused by altitude variations of the AUV above a uniformly magnetized seafloor, we computed a forward model assuming a constant magnetization and the seafloor topography along the tracks of the AUV. The resulting anomalies shows very poor correlation with the observed anomalies. This result is confirmed by the annihilator computed for the area, a distribution of magnetization that produces no magnetic anomaly given the source distribution (mainly the topography) and the AUV tracks (Supplementary Fig. 3). There is no way to obtain a uniform positive magnetization by adding any quantity of this annihilator to the equivalent magnetization computed by inversion of the initial AUV magnetic anomalies (Honsho et al., 2012). On the other hand, the pelagic sediment thickness does probably not exceed 10 to 20 m in the bathymetric lows, as suggested by the small volcanic cones that can still be seen in these areas. We therefore conclude that the observed anomalies cannot be solely ascribed to altitude variations of the AUV above the magnetized basalt, but the basalt magnetization shows significant variations instead. The stronger magnetization generally corresponds to the volcanic highs, and variations seem to exist among the different volcanic edifices, without clear relationship with the volcanic morphology. For instance, the large flat volcano at 178°47'0.3'W and 13°50.6'S shows a strong positive anomaly, whereas a similar flat volcano at 178°45.8'W and 13°50.5'S shows a much lower anomaly. The volcanic region made of small coalescent volcanic cones extending from 178°47.3'W,

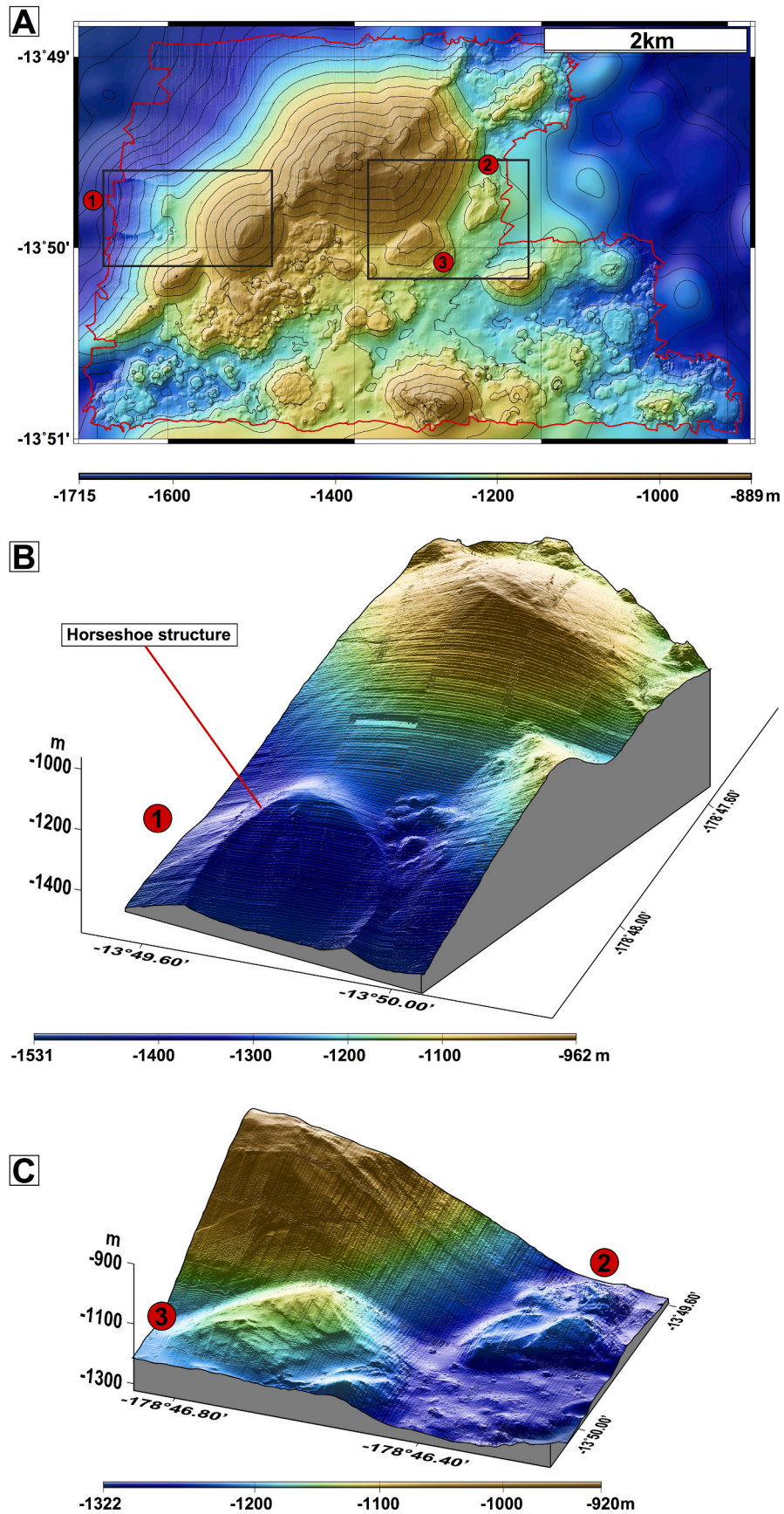


Fig. 2. (A) High-resolution bathymetry of the Utu Uli Hill. The black lines mark the contours of the close-ups in B and C. (B) Close-up on the horseshoe-shape structure sitting on the western slope of the Futuna Ridge. No vertical exaggeration. (C) Close-up on the two slide blocks sitting on the southeastern foot of the Utu Uli Hill.

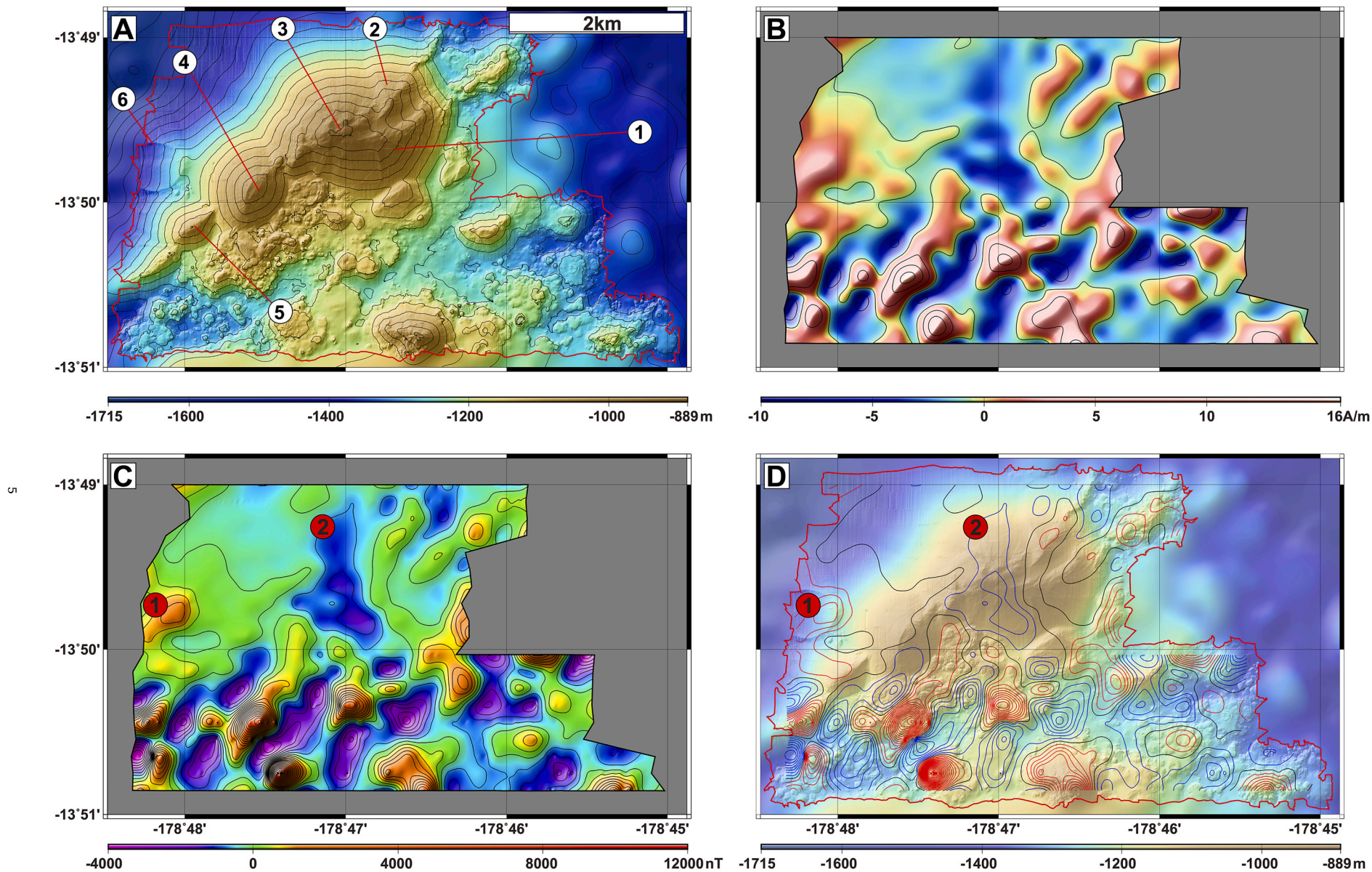


Fig. 3. (A) High-resolution bathymetry of the Utu Uli Hill. Volcaniclastic domes are numbered from 1 to 6. (B) Equivalent magnetization distribution based on [Honsho et al. \(2012\)](#) Bayesian inversion method. (C) Reduced-to-the-Pole (RTP) magnetic anomaly computed from this equivalent magnetization assuming vertical geomagnetic field and magnetization vectors. The crescent-shaped positive magnetic anomaly (marked 1) is associated with the horseshoe collapse structure, and the negative magnetic anomaly (marked 2) corresponds to the Utu Uli Hill summit and may reflect hydrothermal alteration. (D) Contour lines of the RTP magnetic anomaly plotted over the high-resolution bathymetry. Blue (black, red) contours correspond to negative (respectively zero, positive) magnetic anomalies. (For interpretation of the references to colour in this figure legend, the reader is referred to the web version of this article.)

13°49.8'S to 178°48.3'W, 13°50.8'S seems morphologically consistent but displays strong magnetic anomalies at its center around 178°47.5'W, 13°50.4'S and weaker ones at both ends.

The Utu Uli Hill also displays a contrasting magnetic signature, with the central part showing smooth negative RTP anomalies and the northeast and southwest elongated volcanic ridges sharp positive RTP anomalies. The central part is covered by the volcanoclastic sediments, in agreement with its smooth anomalies, and its negative anomaly results from the contrast of magnetization with the nearby basaltic seafloor to the east and south (Fig. 3B, C). At the limit, the two collapse structures flanking the central part to the southeast are characterized by negative RTP anomalies. Conversely, the elongated ridges show outcropping basalt that explain their positive RTP anomalies.

The northwestern sedimented area only shows very weak magnetic anomalies. The RTP anomaly map reveals two major anomalies (Fig. 3C, D). A crescent-shaped positive magnetic anomaly is associated with the horseshoe collapse structure identified on the bathymetry and may correspond to a buried volcanoclastic dome similar to those of the central part of the Utu Uli Hill. A negative magnetic anomaly encompasses the top of the Utu Uli Hill and extends along a north-south direction across the whole central part of the hill over a distance of 1700 m. This anomaly probably reflects the observed volcanic or hydrothermal processes at the origin of the hill. It may either mark the demagnetization of the basaltic basement beneath the hill under temperatures exceeding the Curie temperature of titanomagnetite (~250 °C) (e.g., Kent and Gee, 1996) or the alteration of this basaltic basement by hydrothermal fluid circulation (e.g., Ade-Hall et al., 1971). Thermal anomalies are transient and generally dissipate quite rapidly after eruptions, whereas hydrothermal alteration is permanent (Sztikar et al., 2015). As we lack indication on the age of the last eruption at Utu Uli, this point remains elusive.

4.2. Seismics

East-west Profile (labeled as Inline Profile or IP) 250 (Fig. 4A, B) cuts across the summit of the Utu Uli Hill. As most locations of the seismic survey, it clearly shows the basaltic basement beneath volcanoclastic sediments. Assuming a seismic velocity of 2 km/s for these sediments, the basement depth varies from 320 m beneath the hilltop and progressively decreases to the east. To the west, the sediment thickness rapidly decreases and becomes negligible on the steepest slope whereas it increases and reaches 280 m at the base of the hill. Both ends of the profile display the typical seismic pattern of highly reflective basaltic seafloor. North-south Profile (labeled as Crossline Profile or CP) 550 (Fig. 4A, B) is located ~300 m east of the Utu Uli Hill summit. At its shallowest point, a series of scattered reflections extends from the seafloor over 200 ms. These reflections are also observed on IP250 and define a vertical structure interpreted as the remnant of feeder dykes. Similar volcanic reflections are observed beneath the summit of all volcanoclastic domes. The detailed bathymetry of the volcanoclastic sediment accumulations suggests the presence of different lobes fed by several volcanic edifices. The seismic data confirm this inference and allow us to delimit each volcanoclastic lobe and associate it with its feeder edifice. Figs. 2A and 4B shows the different lobes and their stratigraphic relations, allowing for reconstruction of the progressive building of Utu Uli Hill. The hill is composed of at least four coalescent volcanic edifices (Supplementary Fig. 4) aligned along a SW-NE direction. The stratigraphic relations seem to indicate a south-west propagation of the volcanic activity, i.e. the northeastern volcanic edifices being older than the southwestern one.

The two inferred collapse structures south and east of the Utu Uli Hill central part may also be interpreted as small volcanoes, but their proximity to possible scars on the main structure and the lack of feeder dykes on the seismic data suggests otherwise. The seismic profiles (e.g., IP400 and CP565, respectively; Fig. 4B) clearly show the limits of these slid blocks, which probably corresponds to an intermediate layer of

water-rich disturbed sediments. The half-moon shaped edifice located at the intersection between IP437 and CP757; Fig. 4) also appears to be made of volcanoclastic sediments, with feeder dyke reflections at the top. Its specific geometry suggests that the sediments were preferentially erupted southwards. Despite the lack of seismic coverage for the bathymetric high at 178°46.6 W, 13°50.8S, its shape suggests a similar nature and structure, with the volcanoclastic material preferentially erupted to the north. This edifice is associated with a clear positive magnetic anomaly and may have grown over an older flat-topped basaltic volcano. To summarize, three types of volcanic edifices are observed in the area: ~10 large flat-topped basaltic volcanoes, sometimes covered by small volcanic cones; a 3 km × 1 km region covered by countless small volcanic cones; and two volcanoclastic edifices.

Finally, the horseshoe structure observed to the west shows the combination of a volcanoclastic dome and a collapse structure. Seismic data (e.g., CP158; Fig. 4B) shows feeder dykes where a positive RTP anomaly is also observed (Fig. 3C). The bathymetric and seismic data show that the horseshoe collapse structure exhibits a steep slope westward, and the collapsed material was probably transported outside of the survey area. Noticeably, the present depth of the structure is at and below 1300 m, suggesting that it cannot erupt volcanoclastic sediments anymore.

5. Discussion

Our investigations of Utu Uli Hill confirm that high-resolution bathymetric and magnetic surveys together with high-resolution 3D reflection seismic data represent an efficient set of complementary data to depict the nature and structure of the observed volcanic features and to understand their geologic role in the evolution of the Hill.

Located at the northern edge of the Futuna Ridge northern extension, the Utu Uli Hill initially grew as a set of basaltic N50°E trending ridges similar to the present-day elongated ridges observed on the northeastern and southwestern end of the Hill. A possible scenario is that the basaltic pile reached a certain depth where the hydrostatic pressure became low enough to allow submarine pyroclastic eruptions and lava fountains to exist (e.g., Fisher, 1984), leading to a change in the nature of volcanic products and an accumulation of volcanoclastic sediments. This depth threshold was probably reached asynchronously for the different edifices, with three successive coalescent domes in the central part (domes 1–3 on Fig. 3 and Supplementary Fig. 4), then the southwestern dome of the central part at 13°49.9S, 178°47.6'W (dome 4), and more recently the small southwestern dome at 13°50.2S, 178°48.0'W (dome 5). These five domes form the central part of the Utu Uli Hill and represent the current main source of the sediments (Fig. 1C, 2A). Another partially collapsed volcanoclastic dome associated with the horseshoe structure (dome 6) seems to be the youngest of all. The volcanoclastic domes progressively accumulated and were occasionally affected by flank collapse, resulting in at least two blocks of consolidated volcanoclastic sediments sliding about 200 m down along the southeastern slope and at least one clear landslide scar - the horseshoe structure - along the steeper northwestern slope. At present, only three significant collapse structures are observed, suggesting that the domes are not only made of volcanoclastic sediments, but also of structurally coherent feeder dykes and sills that prevent their destruction (Fig. 4B).

Conversely, volcanism in the southeastern area (which belongs to the Futuna Ridge northern extension) displays a variety of edifices, from big flat volcanoes to series of small craters. The series of small volcanoes flanking Utu Uli Hill immediately to the South exhibits various magnetic anomalies (see above), which suggests that they formed at different ages.

The basaltic edifices located in the southeastern area display various positive magnetic anomalies, whereas bathymetric lows are usually associated with negative anomalies. Because the whole area was formed during the Brunhes normal geomagnetic polarity period (see above), positive anomalies correspond to strong normal magnetization and

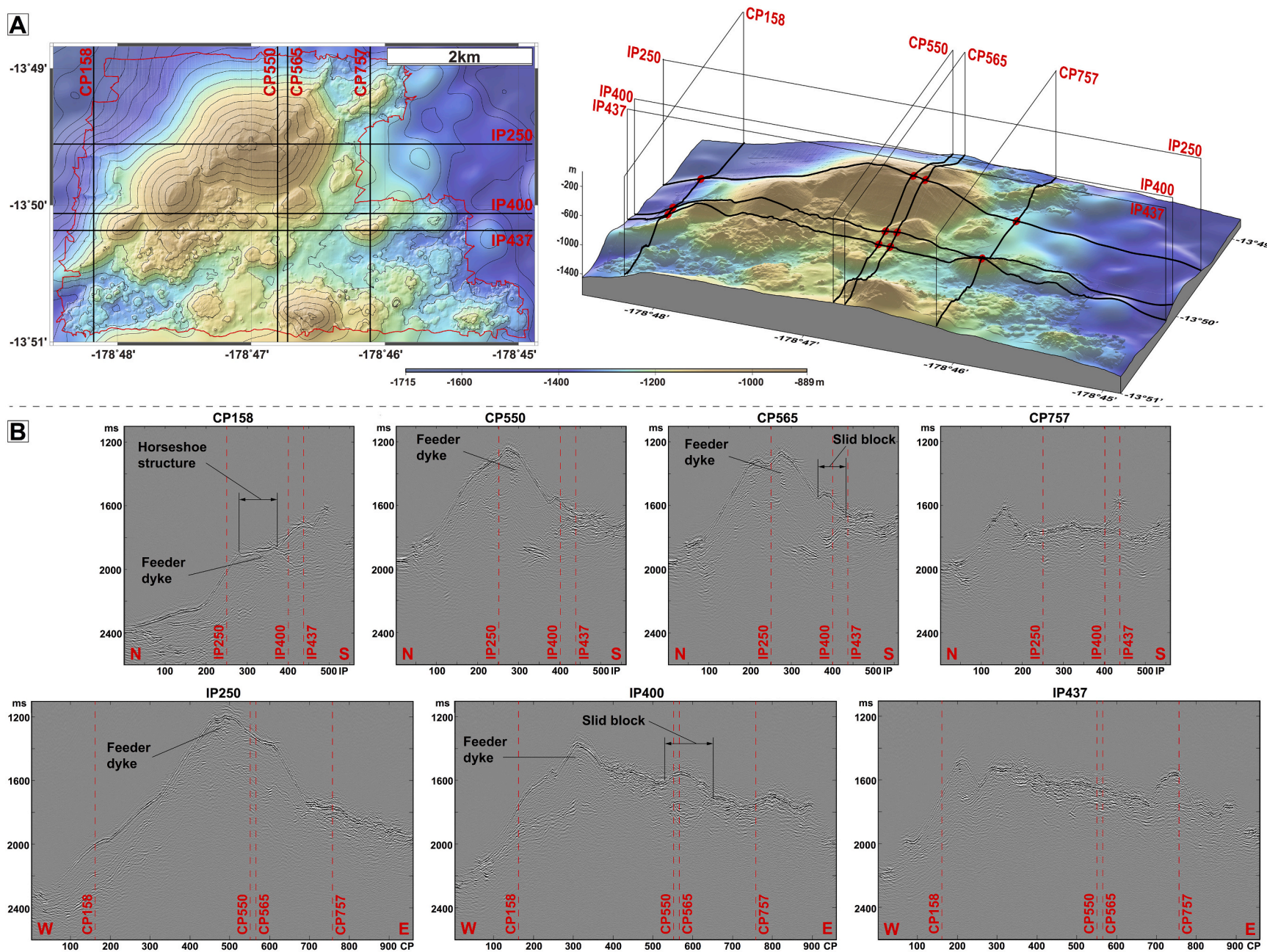


Fig. 4. (A) 2D and 3D projections of the high-resolution bathymetry with representative seismic profiles. (B) Cross-line and In-line seismic profiles, confirming the nature of the slid blocks and unraveling the existence of feeder dykes. The dashed black lines correspond to the upper limit of the basaltic basement below the sediments.

negative anomalies to weak normal magnetization. Beyond the marginal effect of the AUV altitude fluctuations above the magnetized basement, the quite important amplitude variations of magnetic anomalies associated with individual volcanoes may either reflect the effect of alteration, with young fresh lavas being strongly magnetized and older ones seeing their magnetic minerals oxidized and altered by seawater and hydrothermal circulation (e.g., Ade-Hall et al., 1971); or possibly the effect of the geomagnetic field intensity at the time of the lava formation, the magnetization of extrusive basalt reflecting the field paleointensity (e.g., Guyodo and Valet, 1999). Both effects concur for the last 40 ka, since the Laschamp event, i.e. the last geomagnetic paleointensity low (Bonhommet and Zähringer, 1969). More generally, the field has been stronger during the last 10 ka than during the whole Brunhes period (0–780 ka), and stronger during the last 20 ka than during the last 350 ka (e.g., Guyodo and Valet, 1999). We can therefore consider that the stronger anomalies correspond to the younger volcanoes. In this respect, the flat volcano located at 178°47.1 W, 13°50.65S displays almost no magnetic anomaly and is therefore inferred to be among the old ones, whereas those located at 178°47'0.3"W, 13°50.6'S and 178°47.0 W, 13°50.35S show stronger anomalies and are probably more recent. Similarly, the most recent volcanism in the region covered by volcanic cones is probably found around 178°47.5'W, 13°50.4'S (Fig. 3D).

The widespread occurrence of volcanoclastic edifices in the Utu Uli area raises the question of the depth at which explosive eruptions may occur in this area. The central part of the Utu Uli Hill (i.e., the three coalescent domes (domes 1–3) and the isolated southwestern one (dome 4)) and the bathymetric high at 178°46.6'W, 13°50.8'S are well above the 1000 m mark inferred for such eruptions (Fisher, 1984). On the other hand, the small dome further extending the central part to the southwest (dome 5) culminates at 1100 m, the bathymetric high at 178°46.15'W, 13°50.15'S reaches 1180 m, and the top of the horseshoe structure (dome 6) lies at 1280 m. Conversely, the elongated ridges extending the Utu Uli Hill to the southwest and to the northeast culminate between 1220 and 1250 m, suggesting that no volcanoclastic sediment is generated at this depth. These observations suggest that the threshold for pyroclastic eruptions to take place is between 1150 and 1200 m bsl. In a similar context, the West Mata seamount, located 560 km to the east, also shows volcanoclastic deposits emitted at its summit at depths ranging between 1165 and 1205 m, whereas effusive eruptions take place along “rift zones” that resemble our elongated volcanic ridges (Clague et al., 2011; Embley et al., 2014). These depths are very similar to those estimated for the Utu Uli Hill. We anticipate that magma viscosity and gas pressure are important parameters that may affect the threshold above which submarine explosive eruptions may occur.

6. Conclusion

The Utu Uli area displays a variety of submarine volcanic expressions: a cluster of small basaltic volcanoes, basaltic flat-topped volcanoes, basaltic elongated ridges, and volcanoclastic sediment domes. Basaltic volcanoes generally display a strongly reflective (and, when outcropping, diffractive) basement and strong magnetic anomalies. Conversely, volcanoclastic edifices are characterized by seismically transparent bodies, sometimes overlapping a reflective basaltic basement, and show feeder dykes at their summit. They represent magnetically transparent bodies as well and their magnetic anomaly is generally weak, depending on the depth and magnetization of underlying magnetic sources.

Sea-surface magnetic anomalies suggest that the Utu Uli area formed during the Brunhes normal polarity geomagnetic period, which age is younger than 780 ka. The wide range in amplitude of the deep-sea magnetic anomalies associated with basaltic volcanoes reflects the age of these edifices as a result of alteration and paleointensity. Alteration of basalt at the contact of seawater and through hydrothermal circulation progressively degrades magnetic minerals and reduces the basalt

magnetization. Strong and pervasive hydrothermal circulation and the resulting alteration and mineralization are indeed observed near the summit of the Utu Uli Hill (Pelleter et al., 2017), associated with a negative magnetic anomaly. The amplitude of the magnetic anomalies also reflects the geomagnetic intensity at the time of the lava cooling below the Curie temperature, which continuously increased since 40 ka. The strong amplitude variation without any clear geographic distribution suggests that the volcanism is widespread over the Futuna Ridge northern extension and is not limited to a simple plate boundary, as shown for other platelet boundaries in the Lau Basin (Sztikar et al., 2020).

Finally, our work further constrains the depth of the threshold above which pressure conditions allow the existence of submarine pyroclastic eruptions and lava fountains, and the emission of volcanoclastic sediments. This depth, between 1150 and 1200 m, is in good agreement with the depth obtained (1165–1205 m) observed at the West Mata active pyroclastic eruptions.

Declaration of Competing Interest

The authors declare that they have no known competing financial interests or personal relationships that could have appeared to influence the work reported in this paper.

Data availability

The data that has been used is confidential.

Acknowledgements

We thank the captain and crew of R/V *L'Atalante*, the technical teams of AUV *Aster^X* and *Idef^X* and DSV *Nautile*, and the IFREMER scientific team for excellent work at sea during Cruises FUTUNA 2010 and 2012. IGP, CNRS-INSU, IFREMER, and GENAVIR are gratefully acknowledged for their financial and technical support. F.S. was supported by a fellowship funded by IFREMER and CNRS in the early stages of this research. The data presented in this paper have been collected as part of an industrial project and are proprietary. The authors are grateful to Eramet, Technip and Areva. The Geological Survey of Norway (NGU) supported this research. We thank the Editor and the two Reviewers for their useful comments.

Appendix A. Supplementary data

Supplementary data to this article can be found online at <https://doi.org/10.1016/j.jvolgeores.2022.107646>.

References

- Ade-Hall, J.M., Palmer, H.C., Hubbard, T.P., 1971. The magnetic and opaque petrological response of basalt to regional hydrothermal alteration. *Geophys. J. R. Astron. Soc.* 24, 137–174.
- Alken, P., et al., 2021. International Geomagnetic Reference Field: the thirteenth generation. *Earth, Planets and Space* 73 (49). <https://doi.org/10.1186/s40623-020-01288-x>.
- Bonhommet, N., Zähringer, J., 1969. Paleomagnetism and potassium argon age determinations of the Laschamp geomagnetic polarity event. *Earth Planet. Sci. Lett.* 6 (1), 43–46. [https://doi.org/10.1016/0012-821x\(69\)90159-9](https://doi.org/10.1016/0012-821x(69)90159-9).
- Cande, S.C., Kent, D.V., 1995. Revised calibration of the geomagnetic polarity timescale for the late Cretaceous and Cenozoic. *J. Geophys. Res.* 100, 6093–6095.
- Chadwick, W.W., et al., 2008. Direct video and hydrophone observations of submarine explosive eruptions at NW Rota-1 volcano, Mariana arc. *J. Geophys. Res.* 113, B08S10. <https://doi.org/10.1029/2007JB005215>.
- Clague, D.A., Paduan, J.B., Caress, D.W., Thomas, H., Chadwick, W.W., Merle, S.G., 2011. Volcanic morphology of West Mata Volcano, NE Lau Basin, based on high-resolution bathymetry and depth changes. *Geochem. Geophys. Geosyst.* 12, Q0AF03. <https://doi.org/10.1029/2011GC003791>.
- Eissen, J.P., Fouquet, Y., Hardy, D., Ondréas, H., 2003. Recent MORB volcanoclastic explosive deposits formed between 500 and 1750 m.b.s.l. on the Axis of the Mid-Atlantic Ridge, South of the Azores. In: White, J.D.L., et al. (Eds.), *Explosive Subaqueous Volcanism*. AGU.

- Embley, R.W., et al., 2014. Eruptive modes and hiatus of volcanism at West Mata seamount, NE Lau basin: 1996–2012. *Geochem. Geophys. Geosyst.* 15 (10), 4093–4115. <https://doi.org/10.1002/2014GC005387>.
- Fisher, R.V., 1984. Submarine volcanoclastic rocks. *Geol. Soc. Lond. Spec. Publ.* 16, 5–27. <https://doi.org/10.1144/GSL.SP.1984.016.01.02>.
- Fouquet, Y., Eissen, J.P., Ondréas, H., Barriga, F., Batiza, R., Danyushevsky, L., 1998. Extensive volcanoclastic deposits at the Mid-Atlantic Ridge axis: results of deep-water basaltic explosive volcanic activity? *Terra Nova* 10, 286–289.
- Guyodo, Y., Valet, J.P., 1999. Global changes in intensity of the Earth's magnetic field during the past 800 kyr. *Nature* 399 (6733). <https://doi.org/10.1038/20420>.
- Honsho, C., Ura, T., Tamaki, K., 2012. The inversion of deep-sea magnetic anomalies using Akaike's Bayesian information criterion. *J. Geophys. Res.* 117, B01105. <https://doi.org/10.1029/2011JB008611>.
- Kent, D.V., Gee, J., 1996. Magnetic alteration of zero-age oceanic basalt. *Geology* 24, 703–706.
- Lagabrielle, Y., et al., 1996. Active oceanic spreading in the northern North Fiji Basin. Results of the NOFI cruise of R/V L'Atalante. *Mar. Geophys. Res.* 18, 225–247.
- Pelleter, E., Fouquet, Y., Etoubleau, J., Cheron, S., Labanieh, S., Josso, P., Langlade, J., 2017. Ni-Cu-Co-rich hydrothermal manganese mineralization in the Wallis and Futuna back-arc environment (SW Pacific). *Ore Geol. Rev.* 87, 126–146. <https://doi.org/10.1016/j.oregeorev.2016.09.014>.
- Pelletier, B., Lagabrielle, Y., Cabioch, G., Calmant, S., Regnier, M., Perrier, J., 2000. Transpression active le long de la frontière décrochante Pacifique-Australie: les apports de la cartographie multifaisceaux autour des îles Futuna et Alofi (Pacifique sud-ouest), 2000. *Comptes Rendus de l'Académie des Sciences - Series IIA - Earth Planet. Sci.* 331 (2), 127–132. [https://doi.org/10.1016/S1251-8050\(00\)01383-5](https://doi.org/10.1016/S1251-8050(00)01383-5).
- Pelletier, B., Lagabrielle, Y., Benoit, M., Cabioch, G., Calmant, S., Garel, E., Guivel, C., 2001. Newly identified segments of the Pacific-Australia plate boundary along the North Fiji transform zone. *Earth Planet. Sci. Lett.* 193 (3F4), 347–358.
- Sohn, R., et al., 2008. Explosive volcanism on the ultraslow-spreading Gakkel ridge, Arctic Ocean. *Nature* 453 (7199), 1236–1238. <https://doi.org/10.1038/nature07075>.
- Sztikar, F., Petersen, S., Caratori Tontini, F., Cocchi, L., 2015. High-resolution magnetics reveal the deep structure of a volcanic arc-related basalt-hosted hydrothermal site (Palinuro, Tyrrhenian Sea). *Geochem. Geophys. Geosyst.* 16 <https://doi.org/10.1002/2015GC005769>.
- Sztikar, F., Dymant, J., Le Saout, M., Honsho, C., Gente, P., 2016. Dyking at EPR 16°N hypermagmatic ridge segment: insights from near-seafloor magnetics. *Earth Planet. Sci. Lett.* 453, 288–297. <https://doi.org/10.1016/j.epsl.2016.08.020>.
- Sztikar, F., Dymant, J., Fouquet, Y., 2020. Widespread volcanism Southeast of Futuna Island (SW Pacific Ocean): Magnetic dating and regional consequences. *J. Volc. Geotherm. Res.* 406, 107064 <https://doi.org/10.1016/j.volgeores.2020.107064>.
- Thomas, Y., Marsset, B., Westbrook, G., Grall, C., Geli, L., Henry, P., Cifici, G., Rochat, A., Saritas, H., 2012. Contribution of high-resolution 3D seismic near-seafloor imaging to reservoir-scale studies: application to the active North Anatolian Fault, Sea of Marmara. *Near Surface Geophys.* 10 (4), 291–301.